Nuclear Materials and Energy 12 (2017) 341–345

Contents lists available at ScienceDirect

Nuclear Materials and Energy

journal homepage: www.elsevier.com/locate/nme

An analytical expression for ion velocities at the wall including the sheath electric field and surface biasing for erosion modeling at JET ILW

I. Borodkina[a,b,*], D. Borodin[b], S. Brezinsek[b], A. Kirschner[b], I.V. Tsvetkov[a], V.A. Kurnaev[a], V. Bobkov[c], C.C. Klepper[d], A. Lasa[d], C. Guillemaut[e,f], P. Jacquet[f], M.F. Stamp[f], C. Giroud[f], S. Silburn[f], I. Balboa[f], E. Solano[g], JET Contributors[1]

[a] National Research Nuclear University Mephl, Kashirskoe sh., 31, Moscow, Russia
[b] Forschungszentrum Jülich GmbH, Institut für Energie- und Klimaforschung - Plasmaphysik, 52425 Jülich, Germany
[c] Max-Planck-Institut for Plasmaphysik, EURATOM-Assoziation, Garching, Germany
[d] Oak Ridge National Laboratory, Oak Ridge, TN 37831-6169, USA
[e] Instituto de Plasmas e Fusao Nuclear, Instituto Superior Tecnico, Universidade Lisboa, Portugal
[f] CCFE, Culham Science Centre, Abingdon OX14 3DB, United Kingdom
[g] Laboratorio Nacional de Fusion, CIEMAT, 28040 Madrid, Spain

ARTICLE INFO

Article history:
Received 15 July 2016
Revised 7 February 2017
Accepted 18 March 2017
Available online 12 April 2017

Keywords:
Plasma-surface interaction
JET
ITER-like wall
Beryllium
Erosion
Oblique magnetic field
Electric field
ELM

ABSTRACT

For simulation of plasma-facing component erosion in fusion experiments, an analytical expression for the ion velocity just before the surface impact including the local electric field and an optional surface biasing effect is suggested. Energy and angular impact distributions and the resulting effective sputtering yields were produced for several experimental scenarios at JET ILW mostly involving PFCs exposed to an oblique magnetic field. The analytic solution has been applied as an improvement to earlier ERO modelling of localized, Be outer limiter, RF-enhanced erosion, modulated by toggling of a remote, however magnetically connected ICRH antenna. The effective W sputtering yields due to D and Be ion impact in Type-I and Type-III ELMs and inter-ELM conditions were also estimated using the analytical approach and benchmarked by spectroscopy. The intra-ELM W sputtering flux increases almost 10 times in comparison to the inter-ELM flux.

1. Introduction

Modeling is a key tool for understanding observations at the recently installed JET ITER-like wall (JET-ILW) and extrapolation of the obtained knowledge to ITER. The JET-ILW [1] comprises a tungsten (W) divertor and beryllium (Be) main chamber wall thus matching the material configuration planned for ITER. Estimating plasma facing component (PFC) sputtering by plasma ions is an important issue for ITER as erosion determines the life time of PFC, impacts on the tritium retention by co-deposition with Be and leads to an increase of impurities in core plasma and the consequent reduction in fusion plasma performance. For correct calculation of the sputtering yields for PFCs in the presence of an oblique magnetic field the accurate expression for the sheath electric field must be included.

Earlier work [2] has shown that the ICRH (Ion Cyclotron Resonant Heating) enhances erosion at PFCs magnetically connected to active antennas, where electrical effects induced near the wall by the ICRH antenna were treated as an additional biasing. For correct calculation of the sputtering yields for PFCs under these conditions the analytical expression (AE) for the ion velocity at the surface suggested in [3] is modified to take into account the surface biasing (SB) effect. Results are presented in the current paper. The AE has been applied as an improvement to the earlier ERO modeling [2] of RF-enhanced localized erosion at a JET outboard Be limiter magnetically connected to a remote ICRH antenna. By including this effect as an additional negative SB of up to 200 V

* Corresponding author.
E-mail address: ieborodkina@mephi.ru (I. Borodkina).

[1] See F. Romanelli et al., Proc. of the 25th IAEA Fusion Energy Conference 2014, Saint Petersburg, RF

http://dx.doi.org/10.1016/j.nme.2017.03.031

[4] and taking into account an oblique magnetic field we obtained an increase of the local effective sputtering yield by a factor of 2–3. The comparison of the simulated RF-enhanced Be emission with experimental observations and the earlier ERO simulations is presented. Furthermore, a correlation between Be light emission close to the inner wall guard limiter at the mid-plane (solid Be, octant '7X') and the ICRH antenna 'D' is discovered. The possible scenarios behind this effect are discussed. It should be noted that the RF-enhanced Be erosion leads to the increasing of the effective sputtering yield of W surfaces.

Further, W sputtering from divertor plates is expected to be the dominant impurity source during ELMs. The analytical procedure for reproduction of the initial velocity distribution of ions leaving pedestal during ELM based on the "Free-Streaming" model [5] and experimental results is suggested. The linear dependence of the ELM target ion impact energy on the pedestal electron temperature measured in Type-I ELM discharges [6] was extrapolated to lower pedestal temperatures, which correspond to the occurrence of Type-III ELMs. The W sputtering flux due to D^+ and Be^{2+} ion impacts in Type-I and Type-III ELMs and inter-ELM conditions were estimated using the analytic approach [3] and benchmarked by spectroscopy.

2. The analytical expression for the ion motion in the sheath taking into account SB

For modeling of the erosion of the PFC surface with additional surface biasing (further defined as target surface) we take into account the local electric field depending on the surface biasing in the AE for the ion velocity just before the surface impact [3]:

$$\begin{cases} \Delta t_k = \frac{-Vy_k - \sqrt{Vy_k{}^2 - 2(y_k - y_{k+1})(\eta E(y_k) - Vx_k \omega \sin\alpha)}}{(\eta E(y_k) - Vx_k \omega \sin\alpha)} \\ Vx_{k+1} = Vx_k + \omega \cdot \Delta t_k \cdot (Vy_k \cdot \sin\alpha + Vz_k \cdot \cos\alpha) \\ Vy_{k+1} = Vy_k - \eta \cdot E(y_k) \cdot (\Delta t_k) - \omega \cdot \Delta t_k \cdot Vx_k \sin\alpha \\ Vz_{k+1} = Vz_k - Vx_k \cos\alpha \cdot \omega \Delta t_k \end{cases} \quad (1)$$

where Y axes is the surface normal, magnetic field B is in YZ coordinate plane, α is an angle between the magnetic field and the surface normal, $\eta = q/m$, $\omega = qB/Mc$, y_k is a sub-layer coordinate, Δt is a particle transit time in a sub-layer of the sheath. The sheath electric field $E(y)$ is calculated as:

$$E(y) = \frac{kT_e}{qr_d} Q\left(a + 2 \cdot c \cdot \frac{y}{r_d}\right) \exp\left(-a \cdot \frac{y}{r_d} - c \cdot \left(\frac{y}{r_d}\right)^2\right) \quad (2)$$

where parameters a, Q [2], c [7] depend on the dimensionless target potential ψ_t influenced by the value of surface biasing as following:

$$\psi_t = \frac{e(U_t - U_{pl})}{kT_e} = \frac{e(U_{sf})}{kT_e} - \ln\left(\frac{S_t}{S_t + S_{rs}} + \frac{S_{rs}}{S_t + S_{rs}} \exp\left(-\frac{e\Delta U_{bias}}{kT_e}\right)\right) \quad (3)$$

where S_t, S_{rs} are the areas of target surface and return surface, which is the relevant part of the device inner surface wetted with the plasma (the target is isolated from it), U_{pl} is the plasma potential at the sheath/presheath boundary, U_{sf} is surface floating potential relative to U_{pl} ([8] Eq. (2.60)), U_t is a target potential, U_{rs} is a return surface potential, $\Delta U_{bias} = U_t - U_{rs}$ is a negative surface biasing. In Fig. 1 the scheme of potentials is presented. As the area of return surface is usually much larger than target's area ($S_t \ll S_{rs}$), the return surface potential remains equal to the floating potential and the target potential in the presence of SB can be calculated as:

$$\frac{e(U_t - U_{pl})}{k \cdot T_e} = \frac{e(U_{sf})}{kT_e} + \frac{e\Delta U_{bias}}{kT_e}, \quad (4)$$

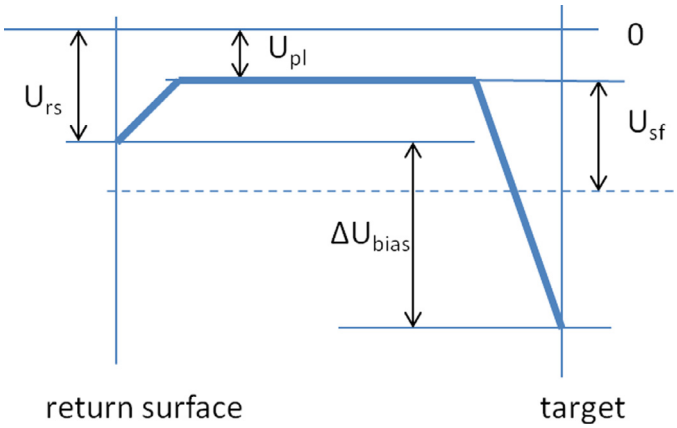

Fig. 1. Scheme of potentials in the presence of the applied surface biasing.

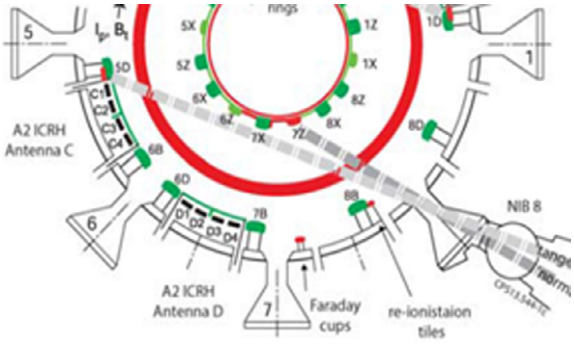

Fig. 2. The JET top view with the considered Be limiters.

3. Simulation of enhanced by RF-emission erosion of JET be limiter

For improving earlier ERO modeling [2] of localized, RF-enhanced, Be outer limiter erosion, modulated by toggling of the remote ICRH antenna 'C', the influence of the oblique magnetic field has been taken into account as well as AE derived above has been applied. The antenna and limiter (solid Be, octant '7B', marked by a circle) considered in the present exercise are shown in Fig. 2. The effect of RF-enhanced erosion has been associated with self-biasing by the intense RF electric fields at the corners of the antenna magnetically connected to the affected limiter. In the modeling, the effect has been represented by an additional negative SB up to −200 V, allowing to interpret the measurements [4]. Fig. 3 presents the sputtering coefficients due to D^+ ions assuming a low-recycling plasma scenario, calculated with the AE and obtained in the earlier simulations, which did not account for the influence of the oblique magnetic field [2]. These sputtering coefficients were calculated assuming 50% D concentration in the surface interaction layer of the Be limiter ('ERO-min' fit [9]). For comparison the case of a pure Be target ('ERO-max' fit) was also calculated with the AE. It is shown that any additional negative surface biasing exceeding −50 V can explain the observed 2–3 fold increase in erosion (characterised by Be spectroscopy) under the 'ERO-min' assumption. This provides additional confidence in 'ERO-min' fit for physical sputtering yields of plasma-wetted areas of PFCs. The updated model leads to an increased effect, which matches the experiment, due to the properly treated angular factor in the sputtering yield.

Similarly to the correlation between Be light emission close to the outer wall guard limiter (7B) and the ICRH antenna 'C' we found a correlation between Be light emission close to the inner

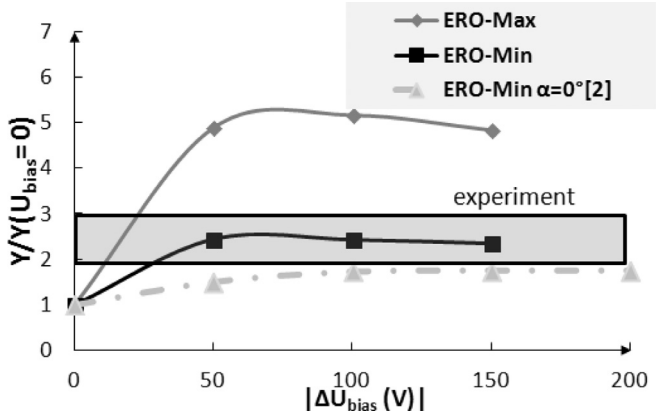

Fig. 3. Comparison of the simulation with AE for different surface content, the earlier ERO modeling (ERO-min for normal incidence) and experimental observations (rectangle) of Be limiter erosion ($\alpha = 85.8°$, B= 1.9T, n=10^{12} cm^{-3}, $T_i = T_e = 5$ eV).

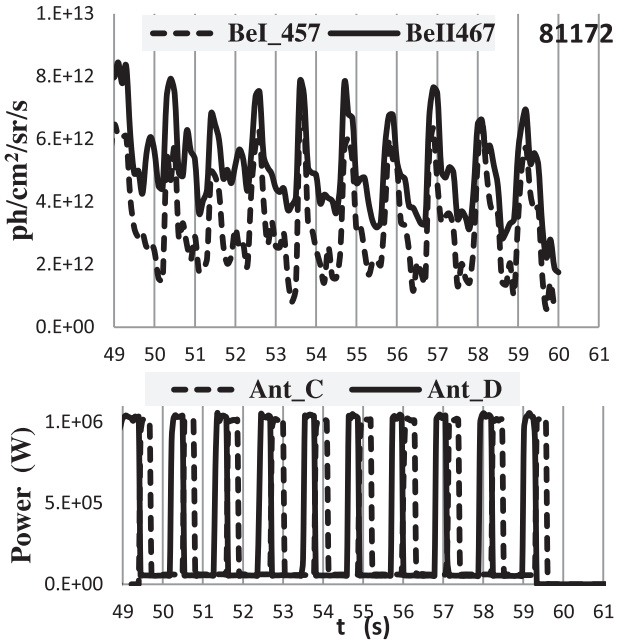

Fig. 4. The enhanced by RF-emission erosion of the Be inner wall guard limiter at the mid-plane (solid Be, octant 7X) modulated by toggling of ICRH antenna 'D'.

wall guard limiter at the mid-plane (octant 7X) and the ICRH antenna 'D' which is presented in Fig. 4. The version of the direct magnetic field connection between antenna and the limiter was checked and declined since multiple tests with a field line tracing program based on EFIT [10] show that a narrow region in front of ICRH antenna connects magnetically to a very broad poloidal and toroidal region at the inner wall. The most probable scenario of this effect is following: more RF-power concentrates in the octant close to the active antenna, the non-absorbed part of RF-power propagating towards the inner wall induces the electric field near inner limiter, opposite the antenna, which leads to sputtering increase similarly to the effect at the outer wall limiter. It should be noted that the value of emission intensity of eroded Be at the inner wall (~7 - 8·10^{12} ph/cm^2/sr/s) is approximately the same as at the outer wall (~5 - 6·10^{12} ph/cm^2/sr/s), although the intensity of RF fields might be different. In both cases the ICRH antenna operation provides 2–3 times sputtering increase. The detailed study of this effect is an issue for further investigation.

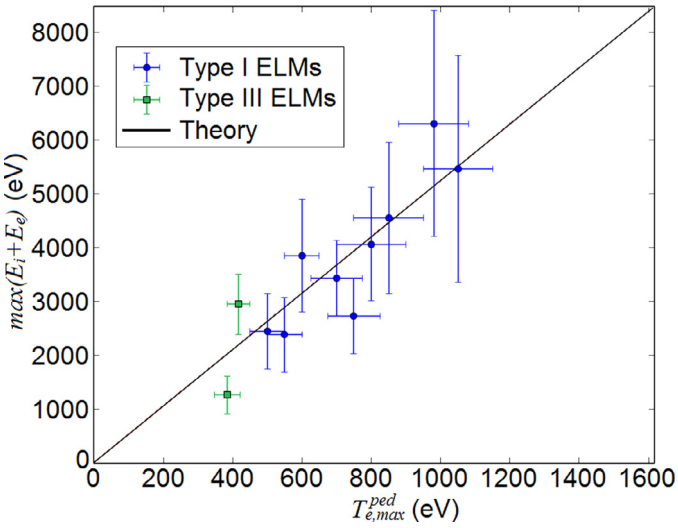

Fig. 5. The ELMy target ion impact energy dependence on the pedestal electron temperature in Type-I and Type-III ELM discharges.

4. Modeling of ion parallel transport and W sputtering yields under intra- and inter-ELM conditions

The new method of estimating the impact energy of deuterium ions (D^+) at a horizontal outer divertor target (OT) using coupled infrared thermography and Langmuir Probe (LP) measurements in JET-ILW unseeded H-mode experiments with ITER relevant ELM energy drop is presented in [6]. It has been established that the ELMy target ion impact energy has a simple linear dependence on the pedestal electron temperature ($T_{e,\max}^{ped}$) measured by Electron Cyclotron Emission (ECE) (Fig. 5) [11] and that the electron temperature close to the target during ELM is low ($T_e \sim 30$ eV). In [12] the W sputtering flux from divertor targets under intra- and inter-ELM conditions was estimated using only the energy at the maximum of the power density. However, for a more detailed estimation the energy and angular distribution of incident ions should be taken into account, therefore it is necessary to determine the initial velocity distribution of ions leaving pedestal during ELMs.

The simulation assumptions were the following. The ions were supposed to start with the modified Maxwell velocity distribution (satisfying the generalized Bohm criterion [13]) with $T_i = \gamma \cdot T_{e,\max}^{ped}$, where parameter γ was selected using two conditions: 1) the resulting profiles of particle flux density at the surface should coincide with the experimental profiles of LP ion saturation current (J_{sat}); 2) the incident ion energy corresponding to the maximum of the perpendicular heat flux density ($q_\perp$) should match the linear dependence on the $T_{e,\max}^{ped}$:

$$E_{i,\max} = (\alpha - 1) \cdot T_{e,\max}^{ped} = 4.23 \cdot T_{e,\max}^{ped} \quad (5)$$

where $\alpha = 5.23$ [6].

Fig. 6 presents the modelled and experimental normalized J_{sat} profiles for Type-I ELM discharge #82237 with $T_{e,\max}^{ped} = 600$ eV, showing a good match when $\gamma = 0.7$. The resulting profile of ELM particle flux at the surface was obtained assuming an uniform ion motion that is similar to the "Free-Streaming" model [5] and is also confirmed by low sheath T_e in the experiment [6]. The duration of ELM pulse at the surface measured by LP is nearly 5 ms (fig. 6). In Fig. 7 one can see that the obtained incident ion energy corresponding to the maximum of the heat flux equals to 2.7 keV which corresponds to the linear dependence (5) for $T_{e,\max}^{ped} = 600$ eV Therefore, using the initial ion velocity distribution function during an ELM described above, we can calculate the ion impact angle and energy distributions and estimate the intra-ELM W effective

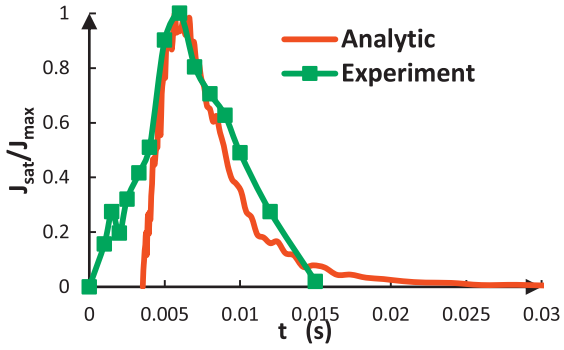

Fig. 6. The modelled and experimental normalized profiles of ion saturation current during ELM ($T_{e,\max}^{ped}$ = 0.6 keV, γ = 0.7).

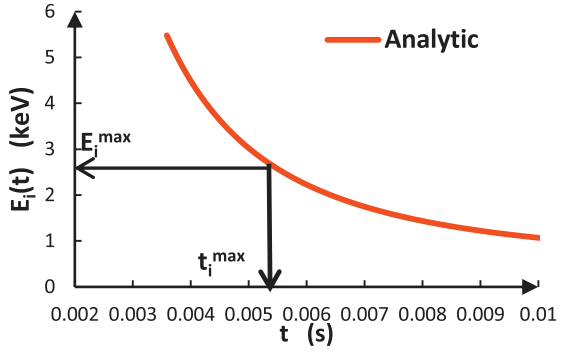

Fig. 7. Time dependence of the ELMy target ion impact energy obtained by the LP – analytic approach ($T_{e,\max}^{ped}$ = 0.6 keV).

sputtering yields due to D^+ and Be^{2+} ($Y_{D/W}$ and $Y_{Be/W}$). Following the previous works [6, 14] the Be intrinsic plasma impurity was assumed to consist mostly of Be^{2+}.

In inter-ELM conditions $Y_{D/W}$ is neglected and only sputtering by Be^+ ions is considered [14]. However, during ELM D^+ ions have sufficient energy to significantly contribute to W sputtering [12]. Using kinetic analytical expressions [3] and the initial velocity distribution presented above the energy and angular distributions of impact ions are obtained. The respective average $Y_{Be/W}$ calculated using the Eckstein formula [15] should be around ~ 0.02 in inter-ELM case (assuming plasma parameters of B = 3 T, $n_e = 10^{13}$ cm^{-3}, $T_i = T_e$ = 23 eV, α = 87°). During ELMs the average W sputtering yield due to Be^{2+} and D^+ should reach $Y_{Be/W}$ ~ 0.39 and $Y_{D/W}$ ~ 0.009 respectively (B = 3T, $n_e = 10^{14}$ cm^{-3}, α = 87°, $T_{e,\max}^{ped}$ = 0.6 keV, $T_{i\,ELM} = \gamma \cdot T_{e,\max}^{ped}$). The Be concentration in the impinging ion flux is expected to be around ~ 0.5% in unseeded JET-ILW Type I ELMy H-mode experiments [14]. The W sputtering fluence during an ELM ($\Delta t_{ELM} = 5\ ms$) $N_{W,ELM}$, and inter-ELM W sputtering flux $\Gamma_{W,inter\text{-}ELM}$ have been calculated as follows:

$$N_{W,ELM} \approx \frac{J_{sat,ELM} - J_{sat,interELM}}{e} \cos\alpha \cdot (Y_{D/W} + 0.005 \cdot Y_{Be/W})\,\Delta t_{ELM} \quad (6)$$

$$\Gamma_{W,inter-ELM} \approx \frac{J_{sat,inter\,ELM}}{e} \cos\alpha \cdot 0.005 \cdot Y_{Be/W} \quad (7)$$

where $J_{sat,ELM} = 0.9 MA/m^2$, $J_{sat,interELM} = 0.4 MA/m^2$, $\alpha = 87^o$ were determined from LP measurements for the discharge #82237 [10].

Finally, OT W sputtering sources retrieved from LP measurements using the analytic approach have been compared to similar estimates made with W I spectroscopy [16]. OT W sputtering fluence per ELM and OT inter-ELM W sputtering flux from both methods are given in Table 1. Discrepancies between amounts obtained from both methods do not exceed a factor ~ 2 during ELM and in inter-ELM. Therefore, the assumptions and approximations made in LP-Analytic approach allow obtaining correct estimates of W sputtering. One can see that the amount of sputtered W during ELM is the same as during 1 s of the tokamak inter-ELM operation. Thus, in the presence of the analyzed ELMs ($\Delta t_{ELM} = 5\ ms$, f = 10 Hz) the W sputtering flux increases almost 10 times in comparison to the inter-ELM flux.

Table 1
OT Type-I ELMy W sputtering fluence and OT inter-ELM W sputtering flux in the discharge #82,237. The ELMy flux is calculated as *ELMy W fluence* multiplied by f_{ELM} plus *Inter-ELM W flux*.

Method	W I spectroscopy [16]	LP - Analytic
ELMy W fluence (atoms/ELM)	$5.7 \cdot 10^{18}$	$8.9 \cdot 10^{18}$
Inter-ELM W flux (atoms/s)	$6.3 \cdot 10^{18}$	10^{19}
ELMy flux / Inter-ELM flux	10	9.9

The W sputtering influx during Type-III ELM discharges (#81881, #81883) was analyzed similarly to Type-I ELM discharges. Fig. 5 shows that the 2 available data points for Type-III ELM discharges also match relatively well the linear dependence of the ELM target ion impact energy on the pedestal electron temperature. Therefore, the same assumption is used as previously for Type I ELMs. The calculations described above were also carried out for the discharge #81,881 (B = 2.4T, α = 88°, $T_{e,\max}^{ped}$ = 450 eV, f = 1250 Hz). The W sputtering fluence during ELM ($\Delta t_{ELM} = 0.35\ ms$) and inter-ELM W sputtering flux is $4.2 \cdot 10^{14}$ atoms/ELM and $5.2 \cdot 10^{16}$ atoms/s, respectively. So, in the presence of such ELMs ($\Delta t_{ELM} = 0.35\ ms$, f = 1250 Hz) the W sputtering intensity increases 10 times in comparison to the inter-ELM conditions. In many cases [17] smaller Type III ELMs do lead to a less prominent effect on erosion. However, it should be noted that similar effect on W erosion for both Type I and Type III ELMs is a peculiarity of the case at hand determined by the high pedestal energy which is high enough to overcome the sputtering threshold of W by D^+ even in TypeIII case.

5. Conclusions

An analytical expression (AE) for the ion velocity just before the surface impact including the local electric field and an optional surface biasing effect is presented in this work. The AE has been applied for improving earlier estimates [2] of RF-enhanced localized erosion at a JET outboard Be limiter magnetically connected to a remote ICRH antenna. It is shown that an additional negative surface bias of more than −50 V can explain the observed 2–3 fold increase in the local erosion (characterised by Be spectroscopy), assuming 50% D concentration in the surface interaction layer. The updated model leads to an increased effect of bias on sputtering respect to earlier estimates [2] due to the properly treated angular factor in the sputtering yield. This studied outboard limiter effect is understood as a result of self-biasing at one flux tube extremity by the intense RF fields at the corners in the “near field region” of the antenna connected at the opposite flux tube extremity.

RF-enhanced Be spectral emission was also observed at a Be inner wall guard limiter, but this time correlated with antenna ‘D’ toggling and independent of magnetic connection (q_{edge} scanning). This inner limiter effect is possibly a similar self-biasing caused by residual RF fields not absorbed in the plasma core and reaching the inner-wall (therefore a “far-field” effect).

The analytical approach for reproduction of initial velocity distribution of ions leaving pedestal during ELMs, based on the “Free-Streaming” model and experimental results, is suggested. Outer divertor target W sputtering flux retrieved from LP measurements and from the analytical approach in Type-I ELM and inter-ELM

conditions is in good agreement within a factor of 2 with the estimates made with W I spectroscopy. The W sputtering fluxes during Type-III ELM discharges were also analyzed using the suggested LP-Analytical approach. It is shown that Type-III ELM discharges also follow the linear dependence of the ELM target ion impact energy on the pedestal electron temperature. In the presence of the analyzed Type-I and Type-III ELMs, the W sputtering flux increases 10 times in comparison to the inter-ELM conditions. Thus, the coupled analytic approach and LP measurements allow estimating W sputtering fluences in unseeded JET-ILW Type-I and Type-III ELMy H-mode experiments.

Acknowledgements

This work has been carried out within the framework of the EUROfusion Consortium and has received funding from the Euratom research and training programme 2014–2018 under grant agreement No 633053 and was supported by contract №14.Y26.31.0008 with the Ministry of Education and Science of the Russian Federation. The views and opinions expressed herein do not necessarily reflect those of the European Commission. This work has been initiated within the MEPhi – FZJ strategic partnership.

References

[1] G.F. Matthews, et al., Phys. Scr. 2011 (2011) 014001.
[2] C.C. Klepper, et al., Phys. Scr. (2016) 014035.
[3] I. Borodkina, Contrib. Plasma Phys. 1 – 6 (2016), doi:10.1002/ctpp.201610032.
[4] V.V. Bobkov, et al., Nucl. Fusion (2010) 11 50 035004.
[5] W. Fundamenski, et al., Plasma Phys. Control. Fusion 48 (2006) 109–156.
[6] C. Guillemaut, et al., Plasma Phys. Control. Fusion (2015) 8 57 085006.
[7] I. Borodkina, et al., J. Phys. (2016).
[8] P. Stangeby, The Plasma Boundary of Magnetic Fusion *Devices*, IOP Publishing Ltd, London, 2000.
[9] D. Borodin, et al., J. Nucl. Mater. 438 (2013) 267–271.
[10] D.P. O'Brien, Nucl. Fusion (1992) 32.
[11] E. de la Luna, et al., Rev. Sci. Instrum. 75 (2004) 3831.
[12] C. Guillemaut, Phys. Scr. (2016) 7 T167 014005.
[13] E.R. Harrison, W.B. Thompson, Proc. Phys. Soc. 74 (1959) 145.
[14] S. Brezinsek, et al., J. Nucl. Mater. 463 (2015) S11–S21.
[15] R. Behrisch, W. Eckstein, Topics Appl.Phys. 110 (2007) 33–187.
[16] G.J. van Rooij, et al., J. Nucl. Mater. 438 (2013) S42–S47 (Supplement).
[17] R. Nea, et al., J. Nucl. Mater. 438 (2013) S34–S41.